frontiers in Materials

ORIGINAL RESEARCH
published: 07 March 2022
doi: 10.3389/fmats.2022.806237

Effect of Ti/Al Ratio on the Elemental Partitioning in the Face-Centered Cubic-Based γ-γ′ Dual-Phase High Entropy Alloy Studied by Atom Probe Tomography

Bin Han[1,2]*, *Feng He*[2,3], *Linfei Xia*[1], *Zhijun Wang*[3] and *Ji Jung Kai*[2,4]

[1]Institute of Atomic and Molecular Science, Shaanxi University of Science and Technology, Xi'an, China, [2]Department of Mechanical Engineering, City University of Hong Kong, Kowloon, Hong Kong SAR, China, [3]State Key Laboratory of Solidification Processing, Northwestern Polytechnical University, Xi'an, China, [4]Centre for Advanced Nuclear Safety and Sustainable Development, City University of Hong Kong, Kowloon, Hong Kong SAR, China

The effect of Ti/Al ratio on the elemental partitioning in the $Ni_2CoFeCrTi_xAl_y$ high entropy alloy was studied by atom probe tomography (APT). The APT results indicate that the γ′ nanoparticles have a composition of $(NiCoFeCr)_3TiAl$ which is independent of Ti/Al ratio. The effect of Ti/Al ratio on the partitioning behaviors of Fe and Cr are significantly different from that of Co. The decreasing of Ti/Al ratio significantly enhanced the incorporation of Fe and Cr into the γ′ nanoparticles. However, the concentration of Co in the γ′ nanoparticles declined with the decrease of Ti/Al ratio.

Keywords: high entropy alloy, γ′ nanoparticles, elemental partitioning, atom probe tomography, Ti/Al ratio

OPEN ACCESS

Edited by:
Zengbao Jiao,
Hong Kong Polytechnic University, Hong Kong SAR, China

Reviewed by:
Bharat Gwalani,
Pacific Northwest National Laboratory (DOE), United States
Li Qian,
City University of Hong Kong, Hong Kong SAR, China

***Correspondence:**
Bin Han
binhan@sust.edu.cn

Specialty section:
This article was submitted to Structural Materials, a section of the journal Frontiers in Materials

Received: *31 October 2021*
Accepted: *24 January 2022*
Published: *07 March 2022*

Citation:
Han B, He F, Xia L, Wang Z and Kai JJ (2022) Effect of Ti/Al Ratio on the Elemental Partitioning in the Face-Centered Cubic-Based γ-γ′ Dual-Phase High Entropy Alloy Studied by Atom Probe Tomography. Front. Mater. 9:806237. doi: 10.3389/fmats.2022.806237

INTRODUCTION

High entropy alloys (HEAs) or multi-component alloys are currently attracting extensive attention from the materials science community due to their excellent properties and potential applications in the aerospace and energy industries. (Gludovatz et al., 2014; Li et al., 2016; Lee et al., 2020; Naeem et al., 2020; Yang et al., 2020; Wang et al., 2021). Particularly, the face-centered-cubic (FCC) HEAs exhibit unique properties such as outstanding ductility, (Otto et al., 2013), high radiation tolerance (Gludovatz et al., 2016) as well as excellent corrosion resistance (Lee et al., 2008). Concerning the engineering applications, however, the FCC HEAs are not strong enough, especially their yield strength is insufficient, which severely limits their applications.

The precipitation strengthening by introducing the dispersed hard nanoparticles such as $L1_2$-structured gamma prime (γ′) or D_{022}-structured gamma double prime (γ″) nanoparticles, into the FCC matrix (γ phase) has been proved to be one of the most promising methods to enhance the strength of the FCC HEAs (Shun et al., 2012; He et al., 2016; Gao et al., 2017; Zhao et al., 2017; Liang et al., 2018; He et al., 2019; Tong et al., 2019; Zhao et al., 2019; Gwalani et al., 2021). It is known that the composition of the γ′ or γ″ nanoparticles plays an important role in the structural stability and mechanical properties of the alloys. For instance, Han et al. found that the Co tends to stabilize the γ′ nanoparticles in the $NiCoFeCrTi_{0.2}$ HEA (Han et al., 2018a). Yang et al. show that the addition of Co and Fe can obviously enhance the ductility of γ′ phase (Yang et al., 2018a). Therefore, it is critical to quantitatively clarify elemental partitioning behaviors in the precipitates-strengthened FCC HEAs. However, this issue is still lack of research due to the difficulty of accurately analyzing the composition of the γ′ nanoparticles embedded in the FCC matrix. Although the

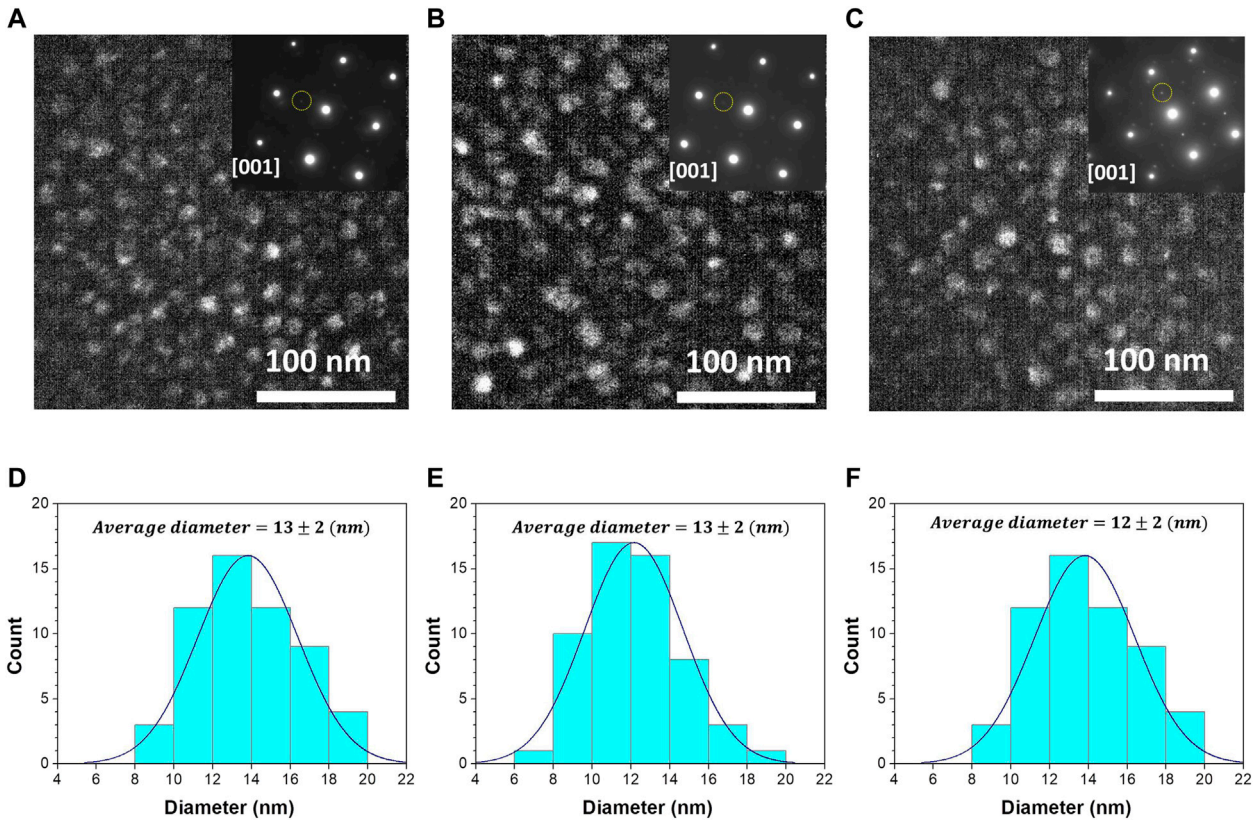

FIGURE 1 | (A–C) The DF-TEM images of the alloy $Ni_2CoFeCrTi_2Al_1$, $Ni_2CoFeCrTi_{1.5}Al_{1.5}$, and $Ni_2CoFeCrTi_1Al_2$ respectively. The insets are the SADP along zone-axis z = [001]. **(D–F)** The size distributions of the γ′ nanoparticles in the corresponding DF-TEM images.

energy-dispersive X-ray spectroscopy (EDS) has been widely approached to study the material composition, it is unable to distinguish the composition of the nanoparticles from the surrounding matrix. Atom probe tomography (APT) is the only technique which can create the three-dimensional (3D) atom maps of materials in the real space with the nearly atomic-scale resolution, which has been proved to be a powerful method of studying the composition of different kinds of nanoparticles (Han et al., 2016; Jiao et al., 2016; Zhao et al., 2017; Han et al., 2018b). Recently, we have successfully approached APT to study the effect of ageing on the partitioning of the alloying elements into the γ′ and γ" nanoparticles in the NiFeCoCr-based HEAs (Han et al., 2018a; Han et al., 2018b). In this work, the effect of Ti/Al ratio on the elemental partitioning in the $Ni_2CoFeCrTi_xAl_y$ HEA was studied by APT. The APT results indicate that the effect of Ti/Al ratio on the partitioning behaviors of Fe and Cr are significantly different from that of Co.

MATERIALS AND METHODS

Three HEA compositions were $Ni_2CoFeCrTi_xAl_y$ (x + y = 0.3, x/y = 2, 1, and 0.5) with the same total Ti and Al concentration and different Al/Ti ratio. The alloy ingots were made in the conventional arc-melting furnace by mixing of pure metals (purity larger than 99.9%). Then, the ingots were drop-casted make slabs with a dimension of 5 × 10 × 50 mm. Afterward, the slabs were treated at 1473 K for 2 h (h) and water quenched to obtain single-phase HEAs. The homogenized slab was cold rolled until the thickness reduced of 80%. Subsequently, they were recrystallized at 1373 K for 5 min and water-quenched. Finally, we performed ageing at 973 K for 24 h.

The transmission electron microscope (TEM) specimen was made by mechanically grinding and ion-milling (PIPS, Model 695, Gatan). The TEM (2100 PLUS, JEOL) was operated under 200 keV. The specimens for APT measurement were made by gallium focused-ion-beam (Scios, FEI) by the conventional lift-out technique. (Miller et al., 2005). The local electrode atom probe (LEAP5000 XR, CAMECA) was used to perform the APT measurement. The voltage mode was run at a specimen temperature of 50 K, and 200 kHz pulses at a pulse fraction of 20%. An Integrated Visualization and Analysis Software (IVAS) protocol was used to analyze the APT data. (Vurpillot et al., 2013).

RESULTS AND DISCUSSION

To confirm the crystal structures and morphologies of the γ′ nanoparticles, the TEM analysis was performed before the APT measurement. **Figures 1A–C** shows the dark field TEM (DF-TEM)

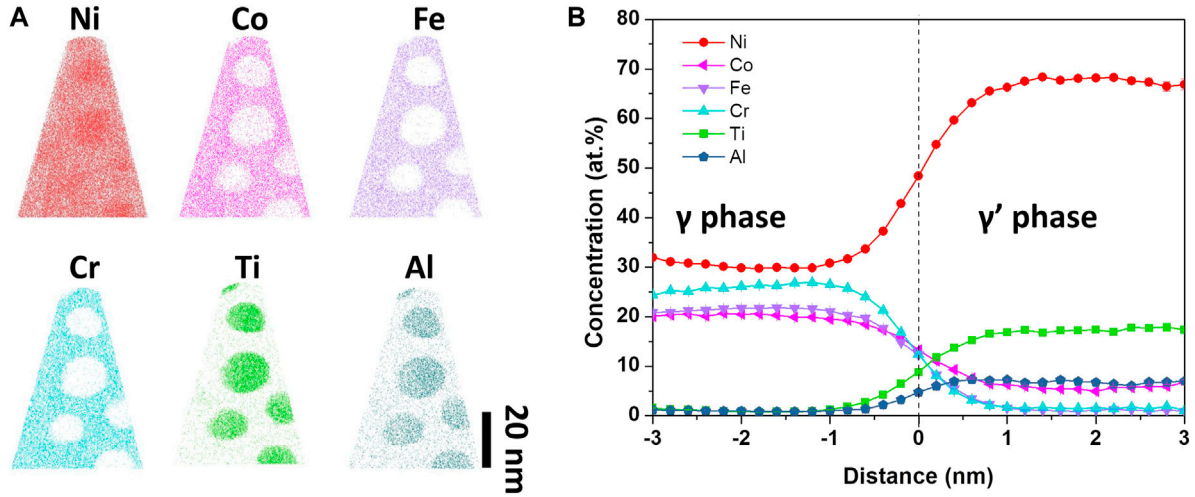

FIGURE 2 | (A) The atom maps of Ni, Co, Fe, Cr, Ti, and Al of the alloy $Ni_2CoFeCrTi_2Al_1$. **(B)** The Proximity histogram of concentration profiles of the γ′ nanoparticles.

images of the alloy $Ni_2CoFeCrTi_2Al_1$, $Ni_2CoFeCrTi_{1.5}Al_{1.5}$, and $Ni_2CoFeCrTi_1Al_2$ which were obtained from superlattice diffraction spots marked with the yellow circles in the inset selected area diffraction patterns (SADP). In the DF-TEM images of the three kinds of the sample, the γ′ nanoparticles with spherical shapes can be clearly observed. Moreover, from the inset SADP along [001] zone axis, it can be confirmed that the matrix has an FCC structure (γ phase), whilst the nanoparticles own a $L1_2$ superlattice structure (γ′ phase). **Figures 1D–F** shows the size distributions of the nanoparticles of the three kinds of alloys. The size of the nanoparticles was measured from the length of the nanoparticles along their long axis in the DF-TEM images using ImageJ software. It can be found that the average nanoparticle size is 13 ± 2 nm in both alloy $Ni_2CoFeCrTi_2Al_1$ and $Ni_2CoFeCrTi_{1.5}Al_{1.5}$, while the average nanoparticle size in alloy $Ni_2CoFeCrTi_1Al_2$ is slightly decreased to 12 ± 2 nm. This result indicated that the average nanoparticle size is almost not affected by the Ti/Al ratio. Moreover, the hardness of the alloys $Ni_2CoFeCrTi_2Al_1$, $Ni_2CoFeCrTi_{1.5}Al_{1.5}$, and $Ni_2CoFeCrTi_1Al_2$ are 352.3, 413.1 and 377.6 HV respectively. Although the nanoparticle sizes are almost the same in the three kinds of alloy, the alloy $Ni_2CoFeCrTi_{1.5}Al_{1.5}$ shows the highest hardness. Furthermore, the nanoparticle shows excellent thermal stability in all the three kinds of alloy, which have been systematically studied in our previous report. (He et al., 2020).

Figure 2 shows the APT results of the elemental partitioning in the alloy $Ni_2CoFeCrTi_2Al_1$. From the atom maps (**Figure 2A**), it can be clearly observed that the γ′ nanoparticles are rich in Ni, Ti, and Al while depleted in Co, Fe, and Cr. The elemental partitioning behavior can be readily extracted from the atom map using the proximity histogram (**Figure 2B**). From the proximity histogram, we can find that the Ni, Ti, Al tend to partition into the γ′ phase, but the Co, Fe, Cr trend to partition into the γ phase. It is worth noting that the Co concentration is much higher than that of Fe and Cr in the γ′ phase, which indicated that Co element shows a stronger tendency to partition into the γ′ phase compared with Fe and Cr. In addition, the APT results also suggested that the γ′ phase is $(NiCoFeCr)_3TiAl$ as the total concentration of Ti and Al in the γ′ phase is 25 at%. This is consistent with our previous results that the γ′ phase with the composition of $(NiCoFeCr)_3Ti$ formed in the $NiCoFeCrTi_{0.2}$ alloy (Han et al., 2018a). Similar elemental partitioning behavior is also observed in the alloy $Ni_2CoFeCrTi_{1.5}Al_{1.5}$, and $Ni_2CoFeCrTi_1Al_2$. **Table 1** summarized the detailed chemical composition of the γ′ nanoparticles and matrix of the three kinds of alloys.

To further study the effect of Ti/Al ratio on the elemental partitioning, the concentration of each element in the γ′ nanoparticles as a function of Ti/Al ratio was depicted in **Figure 3**. As the main composition of the γ′ nanoparticles, the concentration of Ni is almost independent of the Ti/Al ratio. The concentration of Ti decreased and the concentration of Al increased respectively with the decrease of Ti/Al. This is reasonable because Al only substitutes the Ti lattice site in the γ′ nanoparticles, so the change of Ti/Al ratio does not affect the concentration of Ni. In comparison to the main composition of the γ′ nanoparticles, the variation of the depleted elementals (Co, Fe, and Cr) is more interesting. The concentration of Fe and Cr increased dramatically in the γ′ nanoparticles when the Ti/Al ratio decreased. In contrast, the concentration of Co declined in the γ′ nanoparticles with the decrease of Ti/Al ratio. This phenomenon is caused by three reasons. Firstly, Fe and Cr atoms stabilize the Ni_3Al-type γ′ nanoparticles by lowering the valence electron concentration (Yang et al., 2018b). On the other hand, Fe and Cr atoms are rejected from the Ni_3Ti-type γ′ nanoparticles because they cannot form stable chemical bonds with Ti. Thirdly, Co. only tends to stabilize Ni_3Ti-type γ′ nanoparticles by forming strong Co-Ti chemical bonding (Han et al., 2018b). Therefore, the concentration of Fe and Cr increased but Co declined in the γ′ nanoparticles with the decrease of Ti/Al ratio.

In summary, the effect of Ti/Al ratio on the elemental partitioning in the FCC-based γ-γ′ dual-phase $Ni_2CoFeCrTi_xAl_y$ HEA was studied by APT. The measurement of γ′ nanoparticles composition by APT indicates that the γ′ nanoparticles have a composition of

TABLE 1 | Chemical composition of γ′ nanoparticles and matrix (at%).

		Ni	Co	Fe	Cr	Ti	Al
$Ni_2CoFeCrTi_2Al_1$	γ′	68.4 ± 0.16	5.2 ± 0.09	1.0 ± 0.04	0.3 ± 0.03	18.0 ± 0.13	7.0 ± 0.10
	Matrix	33.0 ± 0.4	19.9 ± 0.2	20.2 ± 0.2	23.6 ± 0.2	1.9 ± 0.03	1.4 ± 0.05
$Ni_2CoFeCrTi_{1.5}Al_{1.5}$	γ′	68.8 ± 0.16	4.9 ± 0.09	1.4 ± 0.04	0.5 ± 0.03	15.4 ± 0.13	10.0 ± 0.10
	Matrix	35.9 ± 0.4	18.9 ± 0.2	17.8 ± 0.2	22.7 ± 0.2	2.2 ± 0.03	2.4 ± 0.05
$Ni_2CoFeCrTi_1Al_2$	γ′	67.4 ± 0.16	4.6 ± 0.09	2.0 ± 0.04	0.9 ± 0.03	14.0 ± 0.13	11.1 ± 0.10
	Matrix	37.4 ± 0.4	19.3 ± 0.2	18.0 ± 0.2	21.3 ± 0.2	3.1 ± 0.03	3.5 ± 0.05

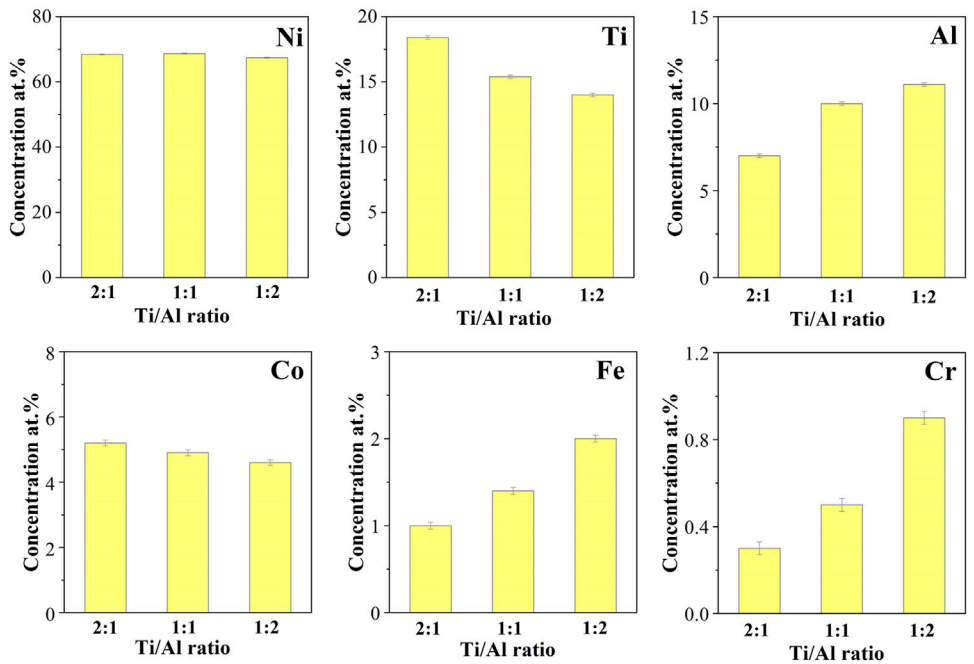

FIGURE 3 | The concentration of each elements in the γ′ nanoparticles as a function of Ti/Al ratio.

$(NiCoFeCr)_3TiAl$ which is independent with Ti/Al ratio. In addition, as the main composition of the γ′ nanoparticles, Ni is almost constant but Ti decreased and Al increased in the γ′ nanoparticles respectively with the decrease of Ti/Al. On the other hand, Fe and Cr increased dramatically but Co declined in the γ′ nanoparticles with the decrease of Ti/Al ratio. Our results are expected to play an important role in the composition control of the γ′ nanoparticles during the HEAs design.

DATA AVAILABILITY STATEMENT

The original contributions presented in the study are included in the article/Supplementary material, further inquiries can be directed to the corresponding author.

AUTHOR CONTRIBUTIONS

BH and FH conceived and designed the experiments. FH designed and prepared the bulk samples. LX prepared the TEM samples. BH performed the APT and TEM experiment and data analysis. BH made the manuscript and discussed with FH, ZW, and JK.

FUNDING

This work was financially supported by the National Natural Science Foundation of China (Nos. 51901119, 51771149, and 52001266), the Hong Kong Research Grant Council (Nos. CityU 11212915 and CityU 11205018), and Natural Science Foundation of ShaanXi Province in China (No. 2020JQ-720).

REFERENCES

Gao, X., Lu, Y., Zhang, B., Liang, N., Wu, G., Sha, G., et al. (2017). Microstructural Origins of High Strength and High Ductility in an AlCoCrFeNi2.1 Eutectic High-Entropy alloy. *Acta Materialia* 141, 59–66. doi:10.1016/j.actamat.2017.07.041

Gludovatz, B., Hohenwarter, A., Catoor, D., Chang, E. H., George, E. P., and Ritchie, R. O. (2014). A Fracture-Resistant High-Entropy alloy for Cryogenic Applications. *Science* 345 (6201), 1153–1158. doi:10.1126/science.1254581

Gludovatz, B., Hohenwarter, A., Thurston, K. V. S., Bei, H., Wu, Z., George, E. P., et al. (2016). Exceptional Damage-Tolerance of a Medium-Entropy alloy CrCoNi at Cryogenic Temperatures. *Nat. Commun.* 7, 10602. doi:10.1038/ncomms10602

Gwalani, B., Dasari, S., Sharma, A., Soni, V., Shukla, S., Jagetia, A., et al. (2021). High Density of strong yet Deformable Intermetallic Nanorods Leads to an Excellent Room Temperature Strength-Ductility Combination in a High Entropy alloy. *Acta Materialia* 219, 117234. doi:10.1016/j.actamat.2021.117234

Han, B., Shimizu, Y., Seguini, G., Arduca, E., Castro, C., Ben Assayag, G., et al. (2016). Evolution of Shape, Size, and Areal Density of a Single Plane of Si Nanocrystals Embedded in SiO_2 Matrix Studied by Atom Probe Tomography. *RSC Adv.* 6 (5), 3617–3622. doi:10.1039/c5ra26710b

Han, B., Wei, J., He, F., Chen, D., Wang, Z., Hu, A., et al. (2018a). Elemental Phase Partitioning in the γ-γ″ $Ni_2CoFeCrNb_{0.15}$ High Entropy Alloy. *Entropy* 20 (12), 910. doi:10.3390/e2012091

Han, B., Wei, J., Tong, Y., Chen, D., Zhao, Y., Wang, J., et al. (2018b). Composition Evolution of Gamma Prime Nanoparticles in the Ti-Doped CoFeCrNi High Entropy alloy. *Scripta Materialia* 148, 42–46. doi:10.1016/j.scriptamat.2018.01.025

He, F., Chen, D., Han, B., Wu, Q., Wang, Z., Wei, S., et al. (2019). Design of D022 Superlattice with superior Strengthening Effect in High Entropy Alloys. *Acta Materialia* 167, 275–286. doi:10.1016/j.actamat.2019.01.048

He, F., Zhang, K., Yeli, G., Tong, Y., Wei, D., Li, J., et al. (2020). Anomalous Effect of Lattice Misfit on the Coarsening Behavior of Multicomponent L12 Phase. *Scripta Materialia* 183, 111–116. doi:10.1016/j.scriptamat.2020.03.030

He, J. Y., Wang, H., Huang, H. L., Xu, X. D., Chen, M. W., Wu, Y., et al. (2016). A Precipitation-Hardened High-Entropy alloy with Outstanding Tensile Properties. *Acta Materialia* 102, 187–196. doi:10.1016/j.actamat.2015.08.076

Jiao, Z. B., Luan, J. H., Miller, M. K., Yu, C. Y., Liu, Y., and Liu, C. T. (2016). Precipitate Transformation from NiAl-type to Ni_2AlMn-type and its Influence on the Mechanical Properties of High-Strength Steels. *Acta Materialia* 110, 31–43. doi:10.1016/j.actamat.2016.03.024

Lee, C., Kim, G., Chou, Y., Musicó, B. L., Gao, M. C., An, K., et al. (2020). Temperature Dependence of Elastic and Plastic Deformation Behavior of a Refractory High-Entropy alloy. *Sci. Adv.* 6 (37), eaaz4748. doi:10.1126/sciadv.aaz4748

Lee, C. P., Chang, C. C., Chen, Y. Y., Yeh, J. W., and Shih, H. C. (2008). Effect of the Aluminium Content of AlxCrFe1.5MnNi0.5 High-Entropy Alloys on the Corrosion Behaviour in Aqueous Environments. *Corrosion Sci.* 50 (7), 2053–2060. doi:10.1016/j.corsci.2008.04.011

Li, Z., Pradeep, K. G., Deng, Y., Raabe, D., and Tasan, C. C. (2016). Metastable High-Entropy Dual-phase Alloys Overcome the Strength-Ductility Trade-Off. *Nature* 534 (7606), 227–230. doi:10.1038/nature17981

Liang, Y.-J., Wang, L., Wen, Y., Cheng, B., Wu, Q., Cao, T., et al. (2018). High-content Ductile Coherent Nanoprecipitates Achieve Ultrastrong High-Entropy Alloys. *Nat. Commun.* 9 (1), 4063. doi:10.1038/s41467-018-06600-8

Miller, M. K., Russell, K. F., and Thompson, G. B. (2005). Strategies for Fabricating Atom Probe Specimens with a Dual Beam FIB. *Ultramicroscopy* 102 (4), 287–298. doi:10.1016/j.ultramic.2004.10.011

Naeem, M., He, H., Zhang, F., Huang, H., Harjo, S., Kawasaki, T., et al. (2020). Cooperative Deformation in High-Entropy Alloys at Ultralow Temperatures. *Sci. Adv.* 6(13): eaax4002. doi:10.1126/sciadv.aax4002

Otto, F., Dlouhý, A., Somsen, C., Bei, H., Eggeler, G., and George, E. P. (2013). The Influences of Temperature and Microstructure on the Tensile Properties of a CoCrFeMnNi High-Entropy alloy. *Acta Materialia* 61 (15), 5743–5755. doi:10.1016/j.actamat.2013.06.018

Shun, T.-T., Chang, L.-Y., and Shiu, M.-H. (2012). Microstructures and Mechanical Properties of Multiprincipal Component CoCrFeNiTix Alloys. *Mater. Sci. Eng. A* 556 (Suppl. C), 170–174. doi:10.1016/j.msea.2012.06.075

Tong, Y., Chen, D., Han, B., Wang, J., Feng, R., Yang, T., et al. (2019). Outstanding Tensile Properties of a Precipitation-Strengthened $FeCoNiCrTi0._2$ High-Entropy alloy at Room and Cryogenic Temperatures. *Acta Materialia* 165, 228–240. doi:10.1016/j.actamat.2018.11.049

Vurpillot, F., Gault, B., Geiser, B. P., and Larson, D. J. (2013). Reconstructing Atom Probe Data: A Review. *Ultramicroscopy* 132, 19–30. doi:10.1016/j.ultramic.2013.03.010

Wang, H., Chen, D., An, X., Zhang, Y., Sun, S., Tian, Y., et al. (2021). Deformation-induced Crystalline-To-Amorphous Phase Transformation in a CrMnFeCoNi High-Entropy alloy. *Sci. Adv.* 7 (14), eabe3105. doi:10.1126/sciadv.abe3105

Yang, T., Zhao, Y. L., Fan, L., Wei, J., Luan, J. H., Liu, W. H., et al. (2020). Control of Nanoscale Precipitation and Elimination of Intermediate-Temperature Embrittlement in Multicomponent High-Entropy Alloys. *Acta Materialia* 189, 47–59. doi:10.1016/j.actamat.2020.02.059

Yang, T., Zhao, Y. L., Liu, W. H., Zhu, J. H., Kai, J. J., and Liu, C. T. (2018a). Ductilizing Brittle High-Entropy Alloys *via* Tailoring Valence Electron Concentrations of Precipitates by Controlled Elemental Partitioning. *Mater. Res. Lett.* 6 (10), 600–606. doi:10.1080/21663831.2018.1518276

Yang, T., Zhao, Y. L., Tong, Y., Jiao, Z. B., Wei, J., Cai, J. X., et al. (2018b). Multicomponent Intermetallic Nanoparticles and Superb Mechanical Behaviors of Complex Alloys. *Science* 362 (6417), 933–937. doi:10.1126/science.aas8815

Zhao, Y. L., Yang, T., Tong, Y., Wang, J., Luan, J. H., Jiao, Z. B., et al. (2017). Heterogeneous Precipitation Behavior and Stacking-Fault-Mediated Deformation in a CoCrNi-Based Medium-Entropy alloy. *Acta Materialia* 138 (Suppl. C), 72–82. doi:10.1016/j.actamat.2017.07.029

Zhao, Y., Yang, T., Han, B., Luan, J., Chen, D., Kai, W., et al. (2019). Exceptional Nanostructure Stability and its Origins in the CoCrNi-Based Precipitation-Strengthened Medium-Entropy alloy. *Mater. Res. Lett.* 7 (4), 152–158. doi:10.1080/21663831.2019.1568315

Conflict of Interest: The authors declare that the research was conducted in the absence of any commercial or financial relationships that could be construed as a potential conflict of interest.